行政院國家科學委員會專題研究計畫　成果報告

低成本之光學感測器研發及應用於碳氫火焰量測

計畫類別：個別型計畫
計畫編號：NSC94-2212-E-216-005-
執行期間：94 年 08 月 01 日至 95 年 08 月 31 日
執行單位：中華大學機械與航太工程研究所

計畫主持人：鄭藏勝

計畫參與人員：趙怡欽 教授、吳志勇(博士後研究員)、李約亨(博士生) 、張智國 (博士生)、楊偉仁(碩士生)

報告類型：精簡報告
報告附件：出席國際會議研究心得報告及發表論文
處理方式：本計畫可公開查詢

中　華　民　國 95 年 11 月 7 日

行政院國家科學委員會補助專題研究計畫 ■ 成 果 報 告 □期中進度報告

低成本之光學感測器研發及應用於碳氫火焰量測
Development of Low Cost Optical Sensors for Hydrocarbon Flame Measurement

計畫類別：■ 個別型計畫　□ 整合型計畫
計畫編號：NSC　94－2212－E －216－005－
執行期間：　94 年　8　月　1 日至　95 年　8　月　31　日

計畫主持人：鄭藏勝 教授
共同主持人：
計畫參與人員：趙怡欽 教授、吳志勇(博士後研究員)、李約亨(博士生）、張智國（博士生)、楊偉仁(碩士生)

成果報告類型(依經費核定清單規定繳交)：■精簡報告　□完整報告

本成果報告包括以下應繳交之附件：
□赴國外出差或研習心得報告一份
□赴大陸地區出差或研習心得報告一份
■出席國際學術會議心得報告及發表之論文各一份
□國際合作研究計畫國外研究報告書一份

處理方式：除產學合作研究計畫、提升產業技術及人才培育研究計畫、列管計畫及下列情形者外，得立即公開查詢
□涉及專利或其他智慧財產權，□一年□二年後可公開查詢

執行單位：中華大學機械與航太工程研究所

中　華　民　國　95　年　11　月　7　日

行政院國家科學委員會九十四年度專題研究計畫成果報告

低成本之光學感測器研發及應用於碳氫火焰量測
Development of Low Cost Optical Sensors for Hydrocarbon Flame Measurement

計畫編號: NSC 94-2212-E-216-005
執行期限: 94 年 8 月 1 日 至 95 年 8 月31 日
主持人:鄭藏勝 中華大學機械與航太工程研究所
E-mail: tscheng@chu.edu.tw

1. 摘要

本計畫預計以三年時間，逐年研發可量測碳氫火焰當量比（混合物分率）、溫度、局部火焰前端厚度與時間尺度、以及火焰速度之低成本無雷射之光學感測器，並應用此診測技術研究紊流預混碳氫火焰其紊流-化學交互作用對污染物生成之影響。由於紊流火焰之污染物生成受局部火焰速度(扭曲率)、局部當量比及溫度之影響相當大，因此，若能同一時間取得上述資訊，則對紊流燃燒污染物生成之機制將會有更深一層的瞭解，進而能即時調整火焰燃燒型態，以降低燃燒污染物生成及提升燃燒效率。但若要同時取得火焰速度(扭曲率)、局部當量比及溫度通常需要使用昂貴的雷射及量測設備，為了發展低成本之量測工具，本計畫第一年(8/2005~7/2006)之研究工作將自行設計組裝兩組具有極佳空間解析度之卡塞格倫反射鏡及兩組光譜分析儀，建立可量測火焰當量比及溫度之無雷射光學感測器，並利用層流預混火焰及部分預混漩渦火焰測試此感測器之準確度及量測紊流火焰之可行性。

關鍵字：低成本光學感測器、卡塞格倫反射鏡、漩渦火焰、自然螢光

2. Abstract

The objectives of this research are to develop low cost, non-laser based optical sensors and to apply these sensors for simultaneous measurements of local flame-front velocity, equivalence ratio (mixture fraction), and temperature in turbulent premixed hydrocarbon flames to investigate the effect of turbulent-chemistry interaction on pollutant formation. The formation of pollutant in turbulent flames is affected by local flame velocity (strain rate), stoichiometry, and temperature. Therefore, simultaneous measurements of quantitative information in turbulent flames not only allow a better understanding of pollutant formation mechanisms but also provide useful information for adjusting combustion status to reduce pollutant emission and increase combustion efficiency. However, it is generally required sophisticated and expensive laser as well as measurement systems to obtain these information simultaneously. Hence, the Principal Investigator proposes this three-year-term's research to develop optical sensor systems in which expensive laser, spectrometers and intensified CCD cameras are excluded. In the first year (8/2005~7/2006), two sets of aberration-free Cassegrain mirrors and spectroscopic analyzers will be developed to test the applicability of the system in laminar premixed and partially premixed swirling flames.

Keywords: Low cost optical sensor, Cassegrain mirror, Swirling flame, Chemiluminescence

3. Introduction

Swirling flows have been widely used in industrial burners in order to increase fuel-air mixing and to improve flame stabilization. It has been shown that swirl can increase mixture homogeneity and shorten the characteristic time for NO_x formation and result in lower NO_x emissions [1-3]. However, in non-premixed swirling flames, the reduction of NO_x emissions is generally accompanied by an increase of CO emissions. Recently, the pollutant emissions generated from *partially premixed swirling* methane jet flames were measured to study the effect of partial premixing on $EINO_x$ and EICO and to develop a scaling law for $EINO_x$ [4]. Measurements indicated that minimization of both NO_x and CO emissions can be achieved with an optimum level of partial premixing in swirling flames. Although similar trend of decrease then increase in $EINO_x$ with increasing levels of partial premixing, as that in laminar flames, was observed in partially premixed swirling methane flames, more information such as radical concentration, reaction rate, and local flame stoichiometry are needed to provide further

explanation of the behaviors in NO_x emissions. The focus of this work is on the measurements of local equivalence ratio in partially premixed swirling flame using non-intrusive method by observing the naturally occurring, optical emissions from the flame.

It has been shown that the chemiluminescent emissions of OH*, CH*, and C_2*, resulted from electronically excited state, in hydrocarbon flames can be related to chemical reaction rate and heat release rate [5-7]. The ratios of chemiluminescence of CH*/OH* and C_2*/OH* were used to determine local equivalence ratio in laminar and turbulent flames [8-9], atmospheric pressure micro-gas turbine combustor [10], and swirl and liquid fuel combustors [11]. Most of these chemiluminescence measurements used traditional lenses to collect the global emissions, and there is insufficient spatial resolution to measure the local equivalence ratio at the flame front. To overcome this deficiency, a Cassegrain optics with high spatial resolution must be used [9, 10, 12]. In the present study, two Cassegrain mirror systems originally designed for Raman scattering measurements [13] are used to simultaneously detect C_2* and OH*/CH* in laminar methane/air flames for calibration purposes. The calibration curve, which is the dependence of OH*/CH* and C_2*/OH* ratio on the equivalence ratio, is then applied for local equivalence ratio measurements in partially premixed swirling flame.

4. Experimental Apparatus

The schematic diagram of the Cassegrain optics is shown in Fig. 1. Cassegrain optics consists of a primary and a secondary mirror, which avoids the generation of chromatic aberrations for different wavelengths. The Cassegrain optics is designed by the ray-tracing method. The designed rms spot size of Cassegrain optics is 328 μm and the magnification ratio is 2.36. The experimental setup is shown in Fig. 2. A Hencken burner is used to produce laminar methane/air flames for the calibration measurements. Chemiluminescence signals emanating from the sample volume are collected and focused by a Cassegrainian optics and relayed to the entrance slit of a 0.275 m, f/3.8 spectrometer (Acton Research Co., SpectraPro-275) with a 1200 grooves/mm grating (3 nm/mm dispersion) and a 0.5 m, f/4 spectrometer (SPEX-500M) with a 1800 grooves/mm grating (1.1 nm/mm dispersion). An intensified CCD camera (Princeton Instruments, 576 x 384 array, 22 x 22 μm pixels) is aligned at the exit plane of the spectrometer for monitoring the emission signals. The measured signals are digitized with a 14-bit A/D card connected to a personal computer for data reduction. The spectral coverage of the 0.275 m spectrometer is 36 nm and that of the 0.5 m spectrometer is 14 nm. The entrance slit of spectrometer is set perpendicular to the flame axial direction. Both spectrometers are aligned by a laser beam to ensure that a same length of 3.34 mm is imaged onto each ICCD camera. This enables the image to be divided into points in the spatial direction to obtain the spatial resolution of measurements. The swirl burner is shown schematically in [4]. A non-swirling axial fuel injector with a swirling co-flowing air stream at S = 1.0 is employed for the present study. The flowrate of fuel and swirling air is respectively kept constant at 8.96×10^{-5} kg/s and 2.41×10^{-3} kg/s for each of the flames while premixed air is added to the fuel stream to manipulate the fuel and swirl-air momentum flux ratio and to change the fuel tube equivalence ratio. The degree of partial premixing in the central fuel tube is indicated by equivalence ratio, Φ_F, of the tube. The inlet temperature of fuel and air is 294 K. The flames are stabilized by the swirling effect. No pilot fuel injection is used.

5. Results and Discussion

In order to study the natural chemiluminescence emission a series of flame emission spectra are taken under several different equivalence ratios. Only the C_2*(0, 0) vibrational band is shown in the paper. The vibrational bands of C_2*(1, 1) and C_2*(0, 0) located at near 513 and 516.5 nm are measured using a 0.5 m spectrometer with 300 μm entrance slit width (as shown in Fig. 3) for Φ = 0.9, 1.1, and 1.4 flames. Although Fig. 3 shows significant background light contributions to C_2*(1, 1) and C_2*(0, 0) bands, their emission intensities are higher than those of C_2*(1, 0) band [9]. Therefore, the C_2*(0, 0) and C_2*(1, 1) bands are used for simulated single-pulse measurements. Under the conditions studied, the profiles of OH*, CH*, and C_2* spectra do not vary much with changes of equivalence ratio. However, the peak intensity of each band spectrum is strongly related to the equivalence ratio. Thus, only the peak intensity of each band spectrum will be used in further studies.

Calibration experiments are performed with the flat-flame burner operated over an equivalence ratio range of 0.8-1.4. For each flame condition, the C_2* (513 and 516.5 nm) and OH* (310 nm) band emission spectrum is simultaneously measured using the 0.5 m and 0.275 m spectrometer, respectively. Then the 0.275 m spectrometer is tuned to 430 nm and kept the 0.5 m spectrometer at the same wavelength for repeated CH* and C_2* measurements. A simulated 200 pulses is recorded for each equivalence ratio. The spectrum is

corrected for background radiation at single-pulse basis. Since the chemiluminescence measurement system collects a length of 3.34 mm of light onto the ICCD camera, the image can be divided into 8 points in the spatial direction to obtain a corresponding spatial resolution of 0.42 mm in the measurements. The dependence of OH*/CH* and C_2*/OH*ratio on the equivalence ratio is respectively shown in Figs. 4 and 5 for 0.42 mm resolution. The intensity ratios are from background corrected, time-averaged peak intensities. In the present study, the calibration is made for each point, i.e., 8 points have 8 calibration curves.

In order to test the ability of the chemiluminescence measurement technique, we apply the calibration curves obtained from laminar flame measurements to a partially premixed swirling flame (Φ_F = 3.1). The measured radial distribution of equivalence ratio at X = 20, 40, 60, and 80 mm is shown in Fig. 6. Experimental results indicate that the measured equivalence ratios at the fuel-side region ($r \leq 2$ mm) are less than those measured at the reaction zone (2 mm < r < 4 mm) for X = 20 and 40 mm. This unrealistic result is due to less OH and C_2 are produced in the fuel-side region of the flame. For further downstream locations (X = 60 and 80 mm), more OH and C_2 are formed in the fuel-side region and result in the measured equivalence ratio of 1.2-1.3.

6. Conclusions

Spatially resolved measurements of flame emission spectra using two Cassegrain mirrors and two spectrometers are performed and used to obtain the correlation of the intensity ratio of OH*/CH* and C_2*/OH* to the equivalence ratio in laminar flames over an equivalence ratio range of 0.8-1.4. The calibration curves are then applied to measure the local equivalence ratio in a partially premixed swirling flame. Experimental results indicate that this non-laser based chemiluminescence technique can only be applied to determine the local flame stoichiometry in the reaction zone of partially premixed swirling methane flames.

7. Self Evaluation

In this project, a low cost optical sensor system has been developed for chemiluminescence measurements in laminar premixed and partially premixed swirling flames. The capability of the developed system has been demonstrated by measuring the local equivalence ratio in a partially premixed swirling flame. Results of this year's research have been published in Combustion Science and Technology (see Appendix). The development of the system for flame-front velocity and temperature is underway.

8. References

[1] Chen, R.-H. (1995) Some Characteristics of NO_x Emission of Turbulent Nonpremixed Hydrogen-Air Flames Stabilized by Swirl-Generated Flow Recirculation. *Combust. Sci. Tech*., **110-111**, 443-460.

[2] Terasaki, T., and Hayashi, S. (1996) The Effects of Fuel-Air Mixing on NO_x Formation in Non-Premixed Swirl Burners. *Proc. Combust. Inst.*, **26**, 2733-2739.

[3] Cheng, T. S., Chao, Y.-C., Wu, D.-C., Yuan, T., Lu, C.-C., Cheng, C.-K., and Chang, J.-M. (1998) Effects of Fuel-Air Mixing on Flame Structures and NO_x Emissions in Swirling Methane Jet Flames. *Proc. Combust. Inst.*, **27**, 1229-1237.

[4] Cheng, T. S., Chao, Y.-C., Wu, D.-C., Hsu, H.-W., and Yuan, T. (2001) Effects of Partial Premixing on Pollutant Emissions in Swirling Methane Jet Flames. *Combust. Flame*, **125**, 865-878.

[5] Gaydon, A. G. and Wolfhard, H. G. *Flames: Their Structure, Radiation, and Temperature*. Fourth edition, Chapman and Hall, 1978.

[6] Lawn, C. J. (2000) Distributions of instantaneous heat release by the cross-correlation of chemiluminescent emissions. *Combust. Flame*, **123**, 227-240.

[7] Najm, H. N., Paul, P. H., Mueller, C. J. and Wyckoff, P. S. (1998) On the adequacy of certain experimental observables as measurements of flame burning rate. *Combust. Flame*, **113** 312-332.

[8] Roby, R. J., Reaney, J .E., and Johnsson, E. L. (1998) Detection of Temperature and Equivalence Ratio in Turbulent Premixed Flames Using Chemiluminescence. *Proceedings of the 1998 International. Joint Power Generation Conference*, **1**, 593-602.

[9] Kojima, J., Ikeda, Y., and Nakajima, T. (2000) Spatially resolved measurement of OH*, CH* and C2* chemiluminescence in the reaction zone of laminar methane/air premixed flames. *Proc. Combust. Inst.*, **28**, 1757-1764.

[10] Hardalupas, Y., Orain, M., Panoutsos, C. S., Taylor, A.M.K.P., Olofsson, J., Seyfrid, H., Richter, M., Hult, J., Aldén, M., Hermann, F. and Klingmann, J. (2004) Chemiluminescence sensor for local equivalence ratio of reacting mixtures of fuel and air (FLAMESEEK). *Appl. Therm. Eng*. **24**, 1619-1632.

[11] Muruganandam, T. M., Kim, B.-H., Morrell, M. R., Nori, V., Patel, M., Romig, B. W. and Seitzman, J. M. (2004) Optical equivalence

ratio sensors for gas turbine combustors. *Proc. Combust. Inst.*, **30**, 1601-1609.

[12] Akamatsu, F., Wakabayashi, T., Tsushima, S., Mizutani, Y., Ikeda, Y., Kawahara, N., and Nakajima, T. (1999) The development of a light-collecting probe with high spatial resolution applicable to randomly fluctuating combustion fields. *Meas. Sci. Technol*. **10**, 1240–1246.

[13] Cheng, T. S., Yuan, T., Chao, Y.-C., Lu, C.-C. And Wu, D.-C. (1998) Premixed methane-air flame spectra measurements using UV Raman scattering. *Combust. Sci. Tech.*, **135**, 65-84.

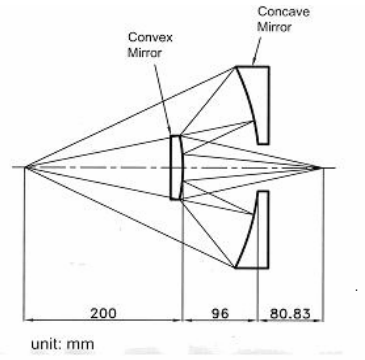

Fig. 1. Schematic diagram of the Cassegrain optics.

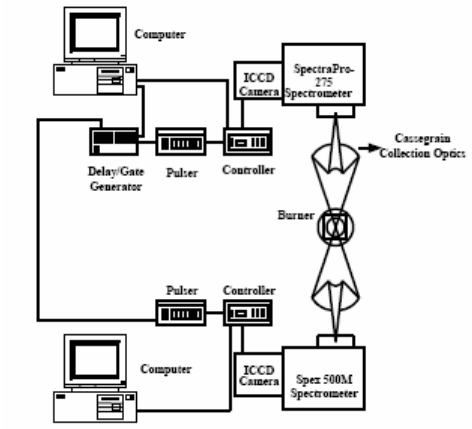

Fig. 2. Experimental setup of measurement system.

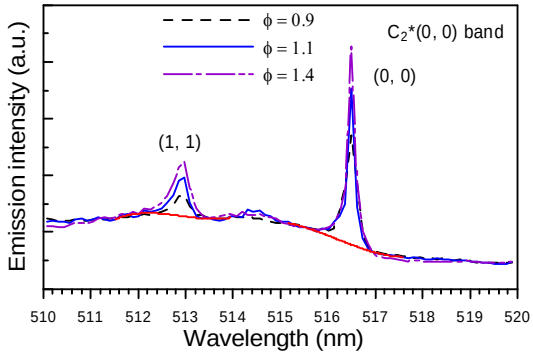

Fig. 3. Flame emission spectra of C_2*(0, 0) band obtained from three different equivalence ratio.

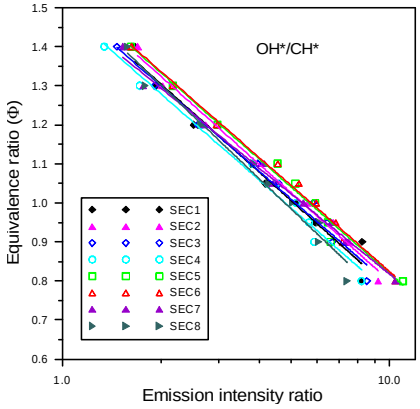

Fig. 4. Correlation of the OH*/CH* intensity ratio to the equivalence ratio.

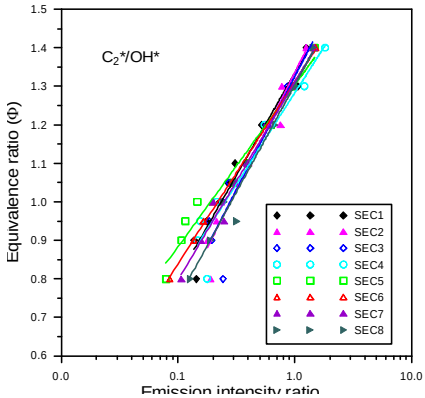

Fig. 5. Correlation of the C_2*/OH* intensity ratio to the equivalence ratio.

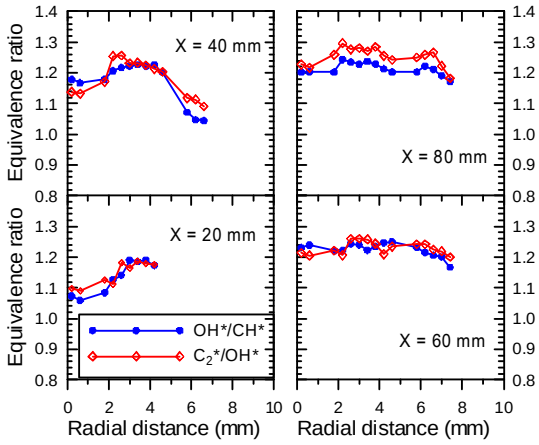

Fig. 6. Time-averaged local equivalence ratio measurements in a partially premixed swirling flame (Φ_F = 3.1).

Combust. Sci. and Tech., 178: 1821–1841, 2006

ISSN: 0010-2202 print/1563-521X online
DOI: 10.1080/00102200600790755

Taylor & Francis
Taylor & Francis Group

CHEMILUMINESCENCE MEASUREMENTS OF LOCAL EQUIVALENCE RATIO IN A PARTIALLY PREMIXED FLAME

T. S. CHENG*

Department of Mechanical Engineering, Chung Hua University, Hsinchu, Taiwan, ROC

C.-Y. WU
Y.-H. LI
Y.-C. CHAO

Department of Aeronautics and Astronautics, National Cheng Kung University, Tainan, Taiwan, ROC

Spatially resolved, time-averaged, multipoint measurements of flame emission spectra using two Cassegrain mirrors and two spectrometers are performed and the results are used to obtain the correlation of the intensity ratio of OH^*/CH^* and C_2^*/OH^* to the equivalence ratio in the laminar flames over an equivalence ratio range of 0.8–1.4. Results show that a strong correlation exists between the intensity ratio and equivalence ratio. The calibration equations obtained from the laminar flame measurements are then applied to obtain the local equivalence ratio in a partially premixed swirling flame. Experimental results demonstrate that multipoint measurement of local equivalence ratio in the partially premixed swirling methane flames is feasible. However, this non-laser based chemiluminescence technique can only be applied to determine the local flame stoichiometry in the reaction zone of the flames. Further improvement of the measurement system and possibility of

Received 4 October 2005; accepted 1 February 2006.

This research was supported by the National Science Council of the Republic of China under Grant numbers NSC 94-2212-E-216-005.

*Address correspondence to tscheng@chu.edu.tw

simultaneous measurements of equivalence ratio and temperature are discussed.

Keywords: chemiluminescence, equivalence ratio, multipoint measurement, partially premixed flame

INTRODUCTION

Swirling flows have been widely used in industrial burners in order to increase fuel-air mixing and to improve flame stabilization. It has been shown that swirl can increase mixture homogeneity and shorten the characteristic time for NO_x formation and result in lower NO_x emissions (Chen, 1995; Terasaki and Hayashi, 1996; Cheng et al., 1998a). However, in non-premixed swirling flames, the reduction of NO_x emissions is generally accompanied by an increase of CO emissions. Recently, the pollutant emissions generated from *partially premixed swirling* methane jet flames were measured to study the effects of partial premixing on emission index of NO_x and CO ($EINO_x$ and EICO) and a scaling law was developed for $EINO_x$ (Cheng et al., 2001). Measurements indicated that minimization of both NO_x and CO emissions can be achieved with an optimum level of partial premixing in swirling flames. Although a similar trend of decrease then increase in $EINO_x$ with increasing levels of partial premixing, as that in partially premixed turbulent jet flames (Lyle et al., 1999), was observed in partially premixed swirling methane flames, more information such as radical concentration, reaction rate, and local flame stoichiometry are needed to understand the effects of mixing and combustion processes on the behavior of NO_x emissions. The focus of this work is to develop a non-intrusive technique using the naturally occurring optical emissions from the flame for the measurement of local equivalence ratio in a partially premixed swirling flame.

In hydrocarbon flames, the chemiluminescent emissions of OH^*, CH^*, and C_2^* resulting from electronically excited states can be related to chemical reaction rate, heat release rate, and equivalence ratio (Gaydon and Wolfhard, 1978; Yamazaki et al., 1990; Najm et al., 1998; Sandrowitz et al., 1998; Lawn, 2000). The chemiluminescence of OH^* and/or CH^* was used for flame detection in combustion turbines (Roby et al., 1995) and for feedback control of equivalence ratio for a continuous combustor (Scott et al., 2000, 2002). The ratios of chemiluminescence of CH^*/OH^* and C_2^*/OH^* were used to determine local

equivalence ratio in laminar and turbulent flames (Roby et al., 1998; Kojima et al., 2000, 2005), atmospheric pressure micro-gas turbine combustor (Hardalupas et al., 2004), and swirl and liquid fuel combustors (Muruganandam et al., 2005). Most of these chemiluminescence measurements used traditional lenses to collect the global emissions, and there is insufficient spatial resolution to measure the local equivalence ratio at the flame front. To overcome this deficiency, Cassegrain optics with high spatial resolution was proposed (Akamatsu et al., 1999; Kojima et al., 2003; Hardalupas et al., 2004).

Although the chemiluminescence measurement techniques have been successfully applied to turbulent flames for determination of local equivalence ratio, most of investigations were made in the "premixed" flames with "single point" measurement. No "multipoint" measurement of local equivalence ratio along a line in the "non-premixed" or "partially premixed" flames has been demonstrated. Multipoint measurement of local equivalence ratio along a line provides instantaneous sensing of stoichiometry across the flame front. In addition, the measured equivalence ratio can be converted to mixture fraction and hence one-dimensional scalar dissipation rates in turbulent flames may be deduced if simultaneous measurement of temperature is made and the time and length scales of the flames can be resolved (Nandula et al., 1994). Therefore, in the present study, the application of a chemiluminescence sensor for multipoint local equivalence ratio measurements in a partially premixed flame is reported. Two Cassegrain mirror systems originally designed for Raman scattering measurements (Cheng et al., 1998b) are used to simultaneously detect C_2^*/OH^* and OH^*/CH^* in laminar methane/air flames for calibration purposes. The calibration equations, which express the dependence of OH^*/CH^* and C_2^*/OH^* ratios on the equivalence ratio, are then applied for local equivalence ratio measurements in a partially premixed swirling flame.

EXPERIMENTAL APPARATUS

Swirl Burner

The schematic diagram of swirl burner is illustrated in Figure 1. A non-swirling axial fuel injector with the swirling co-flowing air stream from six guide vanes at an angle of 55° and geometrical swirl number $S = 1.0$ is employed for the present study. The flowrate of fuel and

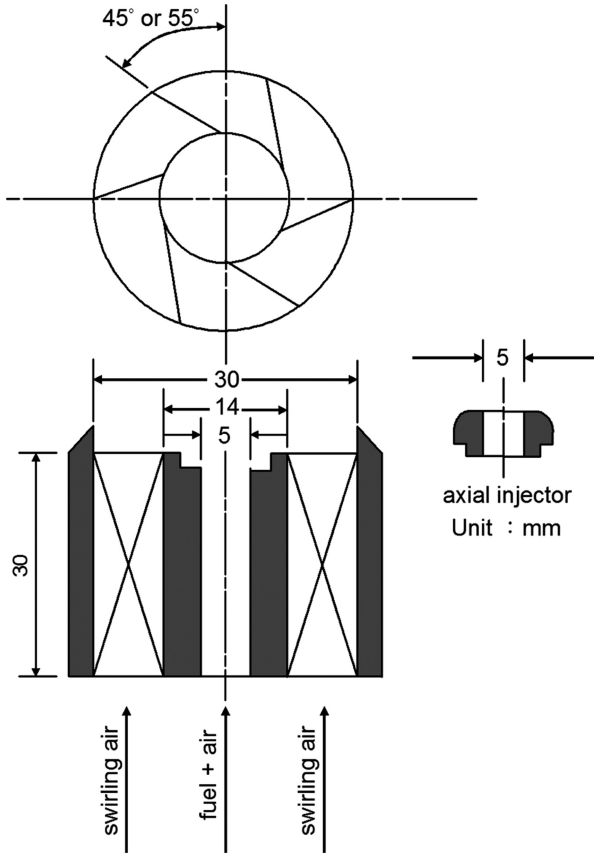

Figure 1. Schematic diagram of swirl burner.

swirling air is respectively kept constant at 8.96×10^{-5} kg/s and 2.41×10^{-3} kg/s, while premixed air is added to the fuel stream to manipulate the fuel and swirl-air momentum flux ratio and to change the fuel tube equivalence ratio. The degree of partial premixing in the central fuel tube is indicated by equivalence ratio, Φ_F, of the tube. The flowrates of methane and air are controlled by mass flowmeters, which have an accuracy of $\pm 1\%$ of full scale with a maximum flowrate of 2.24×10^{-4} kg/s for methane, 1.0×10^{-3} kg/s for premixed air, and 1.0×10^{-2} kg/s for swirling air. The inlet temperature of the fuel and air is 294 K. Flame is stabilized by the swirling effect and no pilot fuel injection is used.

Measurement Systems

The experimental setup of measurement system is shown in Figure 2. The schematic diagram of the Cassegrain optics is also shown in the figure. Cassegrain optics consists of a primary and a secondary mirror, which avoids the generation of chromatic aberrations for different wavelengths. The Cassegrain optics are designed by the ray-tracing method, and its effective probe volume is estimated based on the designed parameters. Since the designed rms spot size (focal point) of Cassegrain optics is 0.328 mm and the magnification ratio is 2.36, thus the theoretical diameter of the sample volume is about 0.14 mm which is comparable to a value of 0.2 mm of the MICRO system (Akamatsu et al., 1999; Kojima et al., 2003). In addition, because the effective width of the ICCD chip is about 7.9 mm, a line-of-light of 3.34 mm ($=7.9\,\text{mm}/2.36$) is imaged from the sample volume. If we divide 3.34 mm by 8 sections, then the spatial resolution across the flame axis is about 0.4 mm. For the estimation of depth of field, we adapt the $f/\#$ of the MICRO system and compare to ours to arrive at the estimation of depth of field. For example, the f number of the primary mirror of MICRO system is $f/\# = 3.013$ (452 mm/150 mm) and the $f/\#$ of ours is $f/\# = 1.6917$ (296 mm/175 mm). Smaller $f/\#$ clearly permits more light to reach the image plane with the same depth of field.

Akamatsu et al. (1999) used a core diameter of 0.2 mm of optical fiber to transmit the light for intensity distribution measurement and they estimated the effective control volume of MICRO system to be 1.6 mm long and 0.2 mm in diameter. Kojima et al. (2003) also used the same MICRO system but with a $d = 0.1$ mm optical fiber and they estimated the effective probe volume to be 0.8 mm in depth and 0.1 mm in diameter. Since the entrance slit height of spectrometer is opened to 0.3 mm for the present study, which is three times the optical fiber diameter used by Kojima et al. (2003). Therefore, the effective cross-section of probe volume of our Cassegrain optics is estimated to be 0.169 mm ($=0.1\,\text{mm} \times 3 \times 1.6917/3.013$) in height and 1.348 mm ($=0.8\,\text{mm} \times 3 \times 1.6917/3.013$) in depth. The estimated height (0.169 mm) of the probe volume is close to the theoretical diameter of 0.14 mm. The estimated effective probe volume for the present Cassegrain optics is $0.4\,\text{mm} \times 0.2\,\text{mm} \times 1.4\,\text{mm}$. Nevertheless, the depth of field (1.4 mm) can be reduced by reducing the slit height or using a 0.1 mm diameter optical fiber for light collection such that the background flame emission

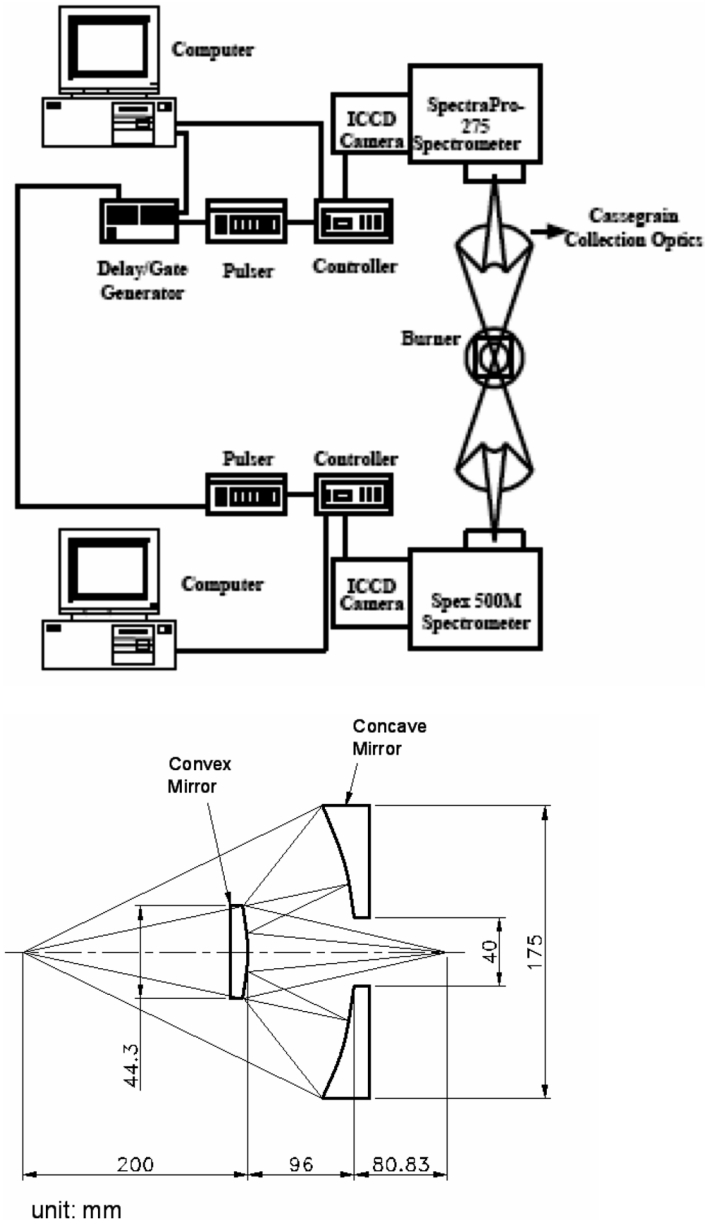

Figure 2. Experimental setup of measurement system and details of Cassegrain optics.

signals collected away from the effective control volume can be greatly reduced.

A flat-flame Hencken burner is operated in a "nonpremixed" mode to produce laminar methane/air flames for the calibration measurements. The burner is composed of fuel tubes distributed in a honeycomb matrix (25.4 mm × 25.4 mm). Air travels through the empty interstices and results in many tiny diffusion flamelets near the surface of the burner. The calibration was made at the center and 5 mm above the burner surface where we believe is in the uniform post-flame zone, though the height is still far from the location of equilibrium post-flame zone (say 3 cm above the burner surface). Chemiluminescence signals emanating from the sample volume are collected and focused by the Cassegrain optics and relayed to the entrance slit of a 0.275 m, f/3.8 spectrometer (Acton Research Co., SpectraPro-275) with a 1200 grooves/mm grating (3 nm/mm dispersion) and a 0.5 m, f/4 spectrometer (SPEX-500M) with a 1800 grooves/mm grating (1.1 nm/mm dispersion). An intensified CCD camera (Princeton Instruments, 576 × 384 array, 22 × 22 μm pixels) is aligned at the exit plane of the spectrometer for monitoring the emission signals. The measured signals are digitized with a 14-bit A/D card connected to a personal computer for data reduction. The spectral coverage of the 0.275 m spectrometer is 36 nm and that of the 0.5 m spectrometer is 14 nm. The entrance slit of spectrometer is set perpendicular to the flame axial direction. Both spectrometers are aligned by a laser beam to ensure that a same length of 3.34 mm is imaged onto each ICCD camera. This enables the image to be divided into points in the spatial direction to obtain the spatial resolution of measurements.

RESULTS AND DISCUSSION

Chemiluminescence Spectra

In order to study the natural chemiluminescence emission a series of laminar flame emission spectra are taken at several different equivalence ratios. Figure 3 shows the typical emission spectra collected in the laminar flames for $\Phi = 0.8$, 1.0, and 1.2 with 1 ms of ICCD camera gate time. The measured spectra are obtained from an average of 200 spectral measurements using a 0.275 m spectrometer with narrow entrance slit (100 μm) to spectrally separate the individual lines. In the spectra, $OH^*(0, 0)$, $OH^*(1, 0)$, $CH^*(0, 0)$, and $C_2^*(1, 0)$ band emissions are clearly

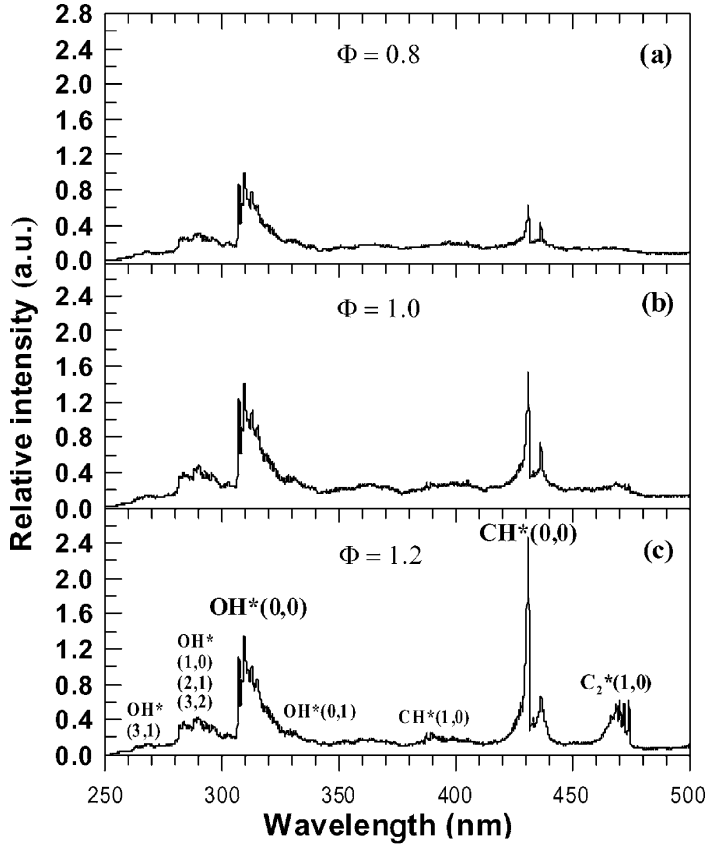

Figure 3. Flame emission spectra measured from laminar methane-air flames at (a) $\Phi = 0.8$, (b) $\Phi = 1.0$, (c) $\Phi = 1.2$.

observed. These emissions are due to following molecular transitions in the flame: OH^* $[A^2\Sigma^+ \rightarrow X^2\Pi]$, CH^* $[A^2\Delta \rightarrow X^2\Pi]$, and $C_2{}^*$ $[A^3\Pi \rightarrow X^2\Pi]$. The CH^* and C_2^* band emissions are more sensitive to variation of the equivalence ratio than is the OH^* emission. The maximum OH^* intensity appears at the stoichiometric condition and the CH^* and C_2^* emission intensities increase as the equivalence ratio increases from lean to rich conditions.

The vibrational bands of $C_2^*(1, 1)$ and $C_2^*(0, 0)$ located near 513 and 516.5 nm are measured using a 0.5 m spectrometer with 300 μm entrance slit width (as shown in Figure 4) for $\Phi = 0.8$, 1.0, and 1.2 flames.

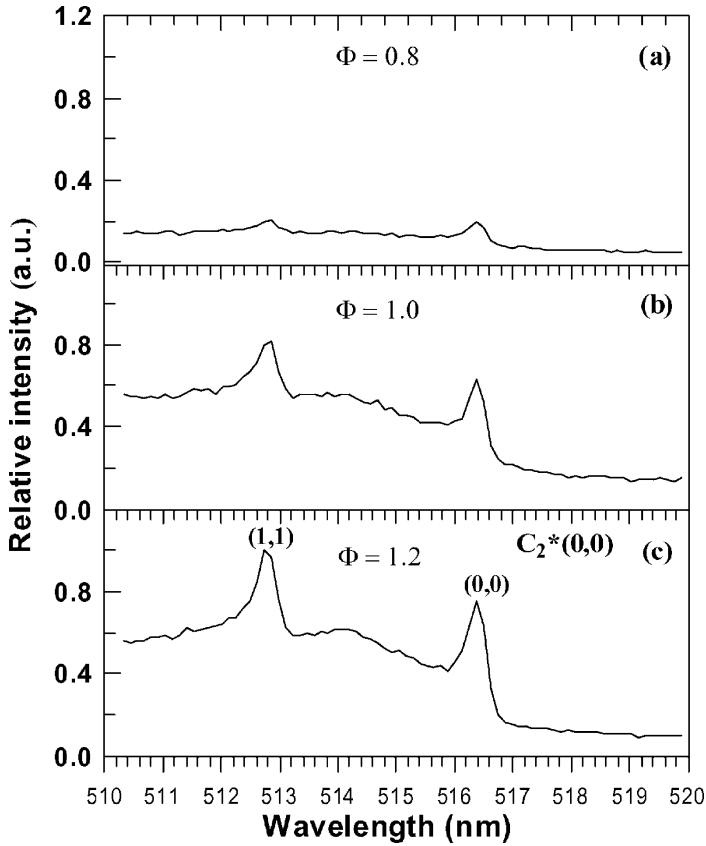

Figure 4. Flame emission spectra of $C_2^*(0, 0)$ band measured from laminar methane-air flames at (a) $\Phi = 0.8$, (b) $\Phi = 1.0$, (c) $\Phi = 1.2$.

Although Figure 4 shows significant background light contributions to $C_2^*(1, 1)$ and $C_2^*(0, 0)$ bands, their emission intensities are higher than those of $C_2^*(1, 0)$ band (Kojima et al., 2000). Therefore, the $C_2^*(0, 0)$ and $C_2^*(1, 1)$ bands (named as C_2^* band) will be used for chemiluminescence emission measurements. In addition, simultaneous monitoring of the $C_2^*(0, 0)$ and $C_2^*(1, 1)$ bands may be used for temperature measurement through the emission intensity ratio of two vibrational bands, if the signal strengths between two bands are strong enough (Ishiguro et al., 1998). Under the conditions studied, the profiles of OH^*, CH^*, and C_2^* spectra do not vary much with changes of equivalence ratio. However, the peak intensity of each band spectrum is strongly related to the

equivalence ratio. Thus, only the peak intensity of each band spectrum will be used in further studies.

Calibration of Measurement System

Calibration experiments are performed with the flat-flame Hencken burner operated over an equivalence ratio range of 0.8–1.4. For each flame condition, the C_2^* (513 and 516.5 nm) and OH^* (310 nm) band emission spectra are simultaneously measured using the 0.5 m and 0.275 m spectrometers each with 300 μm entrance slit width, respectively. Then the 0.275 m spectrometer is tuned to 430 nm and the 0.5 m spectrometer is kept at the same wavelength for repeated CH^* and C_2^* measurements. Since the chemiluminescence measurement system collects a length of 3.34 mm of light onto the ICCD camera, the image can be divided into 16, 8, or 5 points (or sections) in the spatial direction to obtain a corresponding spatial resolution of 0.21, 0.42, or 0.67 mm in the measurements. One of the 8 sections of the OH^*, CH^*, and C_2^* spectra is illustrated in Figure 5.

Several important factors that may affect equivalence ratio measurements in a partially premixed flame are observed from these spatially resolved spectra. Firstly, there is a significant background broadband emission due to chemiluminescence from other sources, such as HCO^* and CO_2^* (Najm et al., 1998; Ikeda et al., 2002). This broadband emission varies with equivalence ratio and is especially significant when the spectral bandwidth of the detection system is broad (Muruganandam et al., 2005). Therefore, to obtain a more accurate measurement of chemiluminescence intensities, background correction based on the side bands must be made. The polynomial fits of the side bands used for background corrections are also shown in the figure. A quadratic or cubic fit to the spectrum around the primary peak is employed, depending on the spectrum of side bands. The curve fit value at $\sim$310 nm is subtracted from the intensity measured, to obtain a corrected OH^* peak intensity, and likewise at $\sim$430 nm for CH^* and $\sim$513 and $\sim$516.5 nm for C_2^*. Secondly, the peak intensity varies with spatial location when the image is divided into sections. The variation of peak intensity is due to non-uniformity of the ICCD detector. This non-uniformity is corrected based on the measured maximum peak intensity to compensate the measured lower intensity and to reduce measurement uncertainty. Then, the calibration is made for each point (section), i.e., 8 points have 8

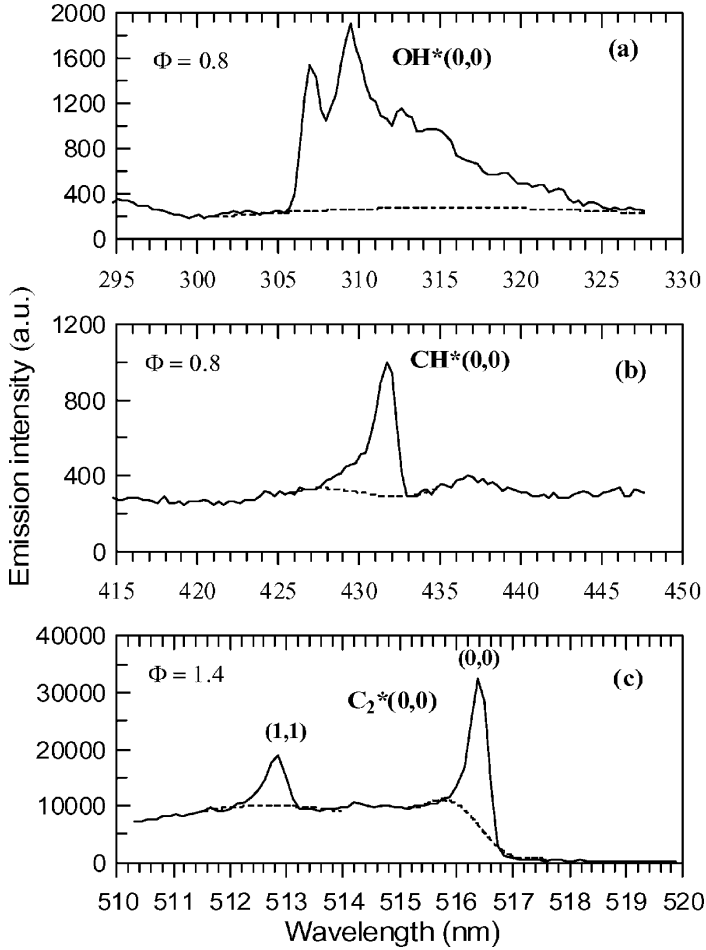

Figure 5. Flame emission spectra of OH^*, CH^*, and C_2^* obtained from one of 8 points and measured in laminar methane-air flames. Dashed lines are the quadratic or cubic fit for background correction used to subtract out the broadband emission.

calibration curves. Last, the wide opened entrance slit width of the detection system allows more light to be measured but degrades the spatial resolution by increasing the depth of field and also results in a broader spectral linewidth (as the detection system employed here). Nevertheless, it has been shown that applying the background correction could significantly improve the sensitivity of the technique (Muruganandam et al., 2005).

To determine suitable spatial resolution for partially premixed flame measurement, the measured calibration spectra are divided into points (or sections) along the slit. Typical comparisons of the dependence of OH^*/CH^* and C_2^*/OH^* ratio on the equivalence ratio with different spatial resolutions in the flame are shown in Figures 6 and 7 for one of the points. Experimental data of Kojima et al. (2005) that were obtained from the laminar CH_4-air premixed flames are also shown in the figures for comparison. The intensity ratios are calculated from the time-averaged peak intensities that are corrected for background and detector non-uniformity. It can be seen that the OH^*/CH^* ratio increases monotonically with decreasing equivalence ratio over the range studied here for three different spatial resolutions (Figure 6), while a different trend is observed for the C_2^*/OH^* ratio (Figure 7). Results of Kojima et al. (2005) also show similar trend of the dependence of intensity ratio on the equivalence ratio. It is noted that due to different types of flame and detector are employed in the present study, the intensity ratio of OH^*/CH^* is divided by a scale factor of 3 to have a better visual

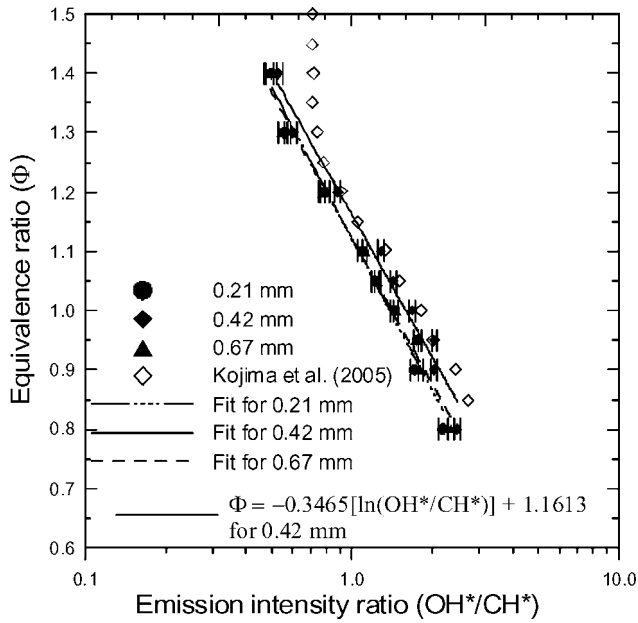

Figure 6. Comparison of the dependence of OH^*/CH^* ratio on equivalence ratio for three different spatial resolutions.

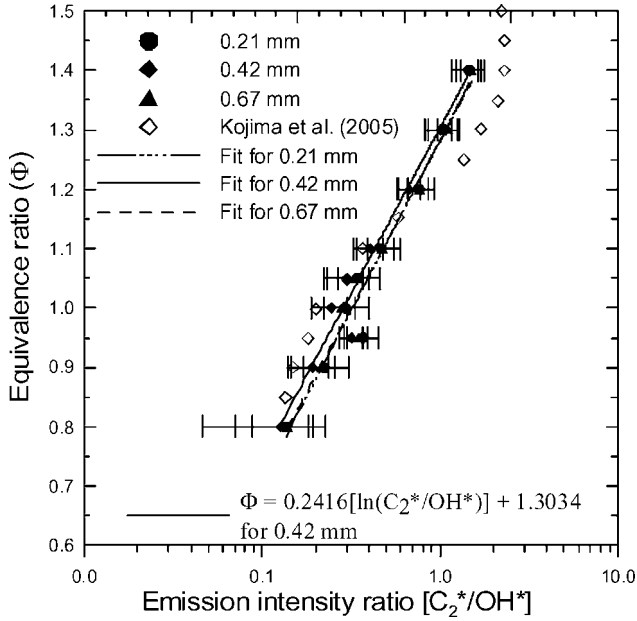

Figure 7. Comparison of the dependence of C_2^*/OH^* ratio on equivalence ratio for three different spatial resolutions.

comparison with the data of Kojima et al. (2005). In all three spatial resolutions, the 0.42 mm resolution shows the greatest sensitivity, and appears to be the best candidate for determining equivalence ratio.

Although the 0.21 mm has twice better resolution than that of 0.42 mm, the uncertainty of intensity ratio is about twice as large. In addition, the spatial resolution of 0.67 mm gives higher signal-to-noise ratio than those of 0.4 mm. However, due to non-uniformity of the CCD chip, the integrated peak signals (after binning process) do not increase linearly proportional to the increased spatial resolution. Therefore, we found that the spatial resolution with largest slope (best sensitivity) for our present measurement system is 0.4 mm. The log curve fit equation of the dependence of OH^*/CH^* and C_2^*/OH^* on the equivalence ratio for the 0.42 mm resolution is also shown in Figures 6 and 7, respectively. These curve fit equations will be used for equivalence ratio measurements in the turbulent flame.

The dependence of OH^*/CH^* and C_2^*/OH^* on the equivalence ratio for 8 sections (0.42 mm resolution) is respectively shown in Figures 8 and 9.

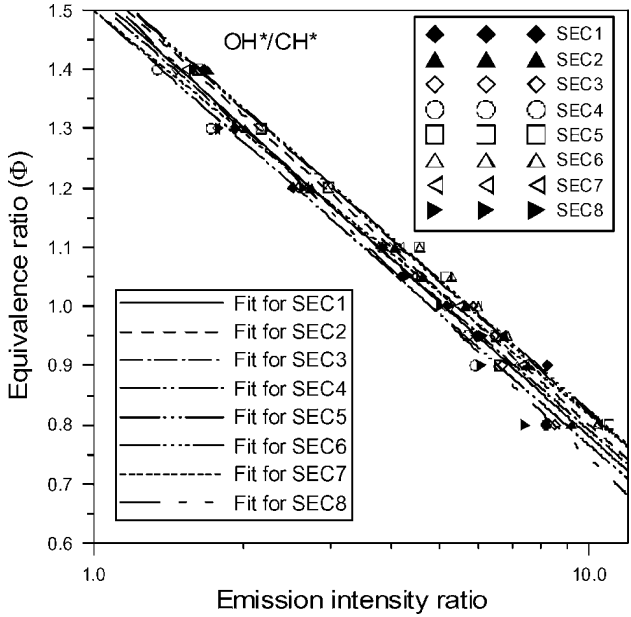

Figure 8. Correlation of the OH^*/CH^* intensity ratio to the equivalence ratio.

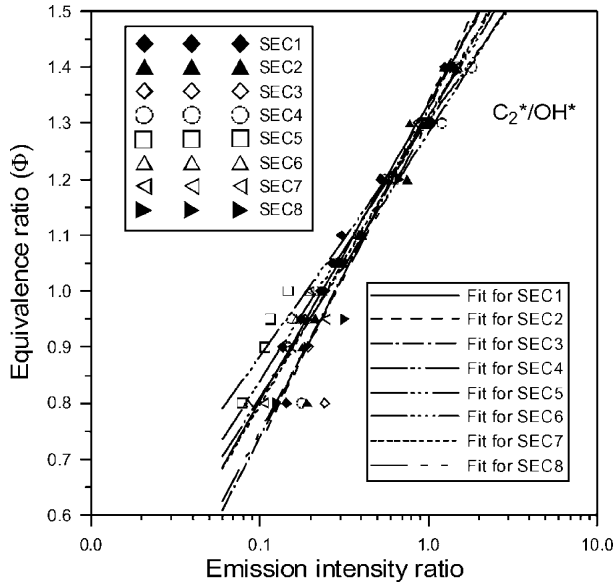

Figure 9. Correlation of the C_2^*/OH^* intensity ratio to the equivalence ratio.

It is noted that the greater scattering of data points at $\Phi = 0.8$ is due to lower chemiluminescence emission of CH^* and C_2^*. This means that this technique would lead to greater uncertainties in equivalence ratio measurements if the local equivalence ratio is less than 0.9. Nevertheless, the high degree of correlation indicates that the local equivalence ratio at the flame front can be determined by spatially resolved chemiluminescence measurements. In the same manner, equations for prediction of the local equivalence ratio can be derived from the curve fit of data points for each section, similar to those presented in Figures 6 and 7. For all calibration conditions and for a given value of equivalence ratio, the OH^*/CH^* and C_2^*/OH^* ratio is within $\pm 10\%$ of the value given by each curve fit equation, which leads to an uncertainty of approximately ± 0.1 for determination of equivalence ratio for $0.9 \leq \Phi \leq 1.4$. It should be noted that the uncertainty of our measurement system is approximately twice as large as those reported by Kojima et al. (2000) and Hardalupas et al. (2004), due to lower quantum efficiency of the ICCD detectors used in this study.

Measurements of a Partially Premixed Swirling Flame

Prior to applying the technique described above for equivalence ratio measurements in the partially premixed swirling flame, the global picture of the flame is presented first. Figure 10 illustrates video and natural chemiluminescence emission images of a partially premixed swirling flame ($\Phi_F = 3.1$). The photograph shows that the flame exhibits blue color, indicating elimination of soot particles by partial premixing. It has been shown that the colors of the partially premixed swirling methane flames became completely blue at $\Phi_F = 4.5$ (Cheng et al., 2001), close to the value of 5 observed in laminar methane flames (Gore and Zhan, 1996). The blue color with increasing premixing in methane flames is attributed to an increase in CH radicals (Gaydon and Wolfhard, 1978). Chemiluminescence emission images of CH^*, C_2^*, and OH^* are respectively taken by placing an interference bandpass filter in front of the ICCD camera. The center wavelength, half-band width, and transmitting efficiency of the optical filters for CH^*, C_2^*, and OH^* measurements are 430 nm/10 nm/40%, 510 nm/10 nm/45%, and 307.1 nm/10 nm/15%, respectively. The instantaneous CH^* distribution is in qualitative agreement with photograph observation. The distributions of CH^*, C_2^*, and OH^* intensities indicate that the ratio of chemiluminescence emission may be used for equivalence ratio measurements in this flame.

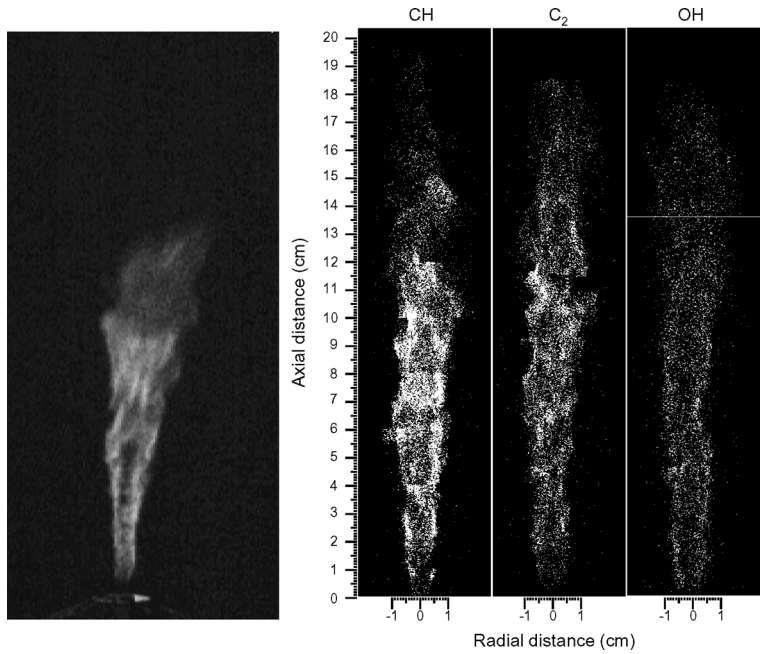

Figure 10. Photograph and CH^*, C_2^*, and OH^* chemiluminescence emission images of a partially premixed methane swirling flame ($\Phi_F = 3.1$).

It is noted that the lower intensity of OH^* than those of CH^* and C_2^* is due to lower transmittance of the optical filter, not to the lower concentration of the excited state OH radicals in the flame.

To test the applicability of the chemiluminescence measurement technique in turbulent flames, we apply the calibration curves obtained from laminar flame measurements to a partially premixed swirling flame ($\Phi_F = 3.1$). The measured radial distributions of time-averaged equivalence ratio at X = 20, 40, 60, and 80 mm are shown in Figure 11. Experimental results indicate that the measured equivalence ratios at the fuel-side region ($r \leq 2$ mm) are less than those measured at the reaction zone (2 mm $< r <$ 4 mm) for X = 20 and 40 mm. These unrealistic results are due to the fact that less OH^* and C_2^* emissions were produced in the central fuel-rich region of the flame. Further downstream locations (X = 60 and 80 mm), more OH^* and C_2^* are formed in the fuel-side region and an equivalence ratio of 1.2–1.3 is measured. The slightly increased equivalence ratio (from 1.24 to 1.28) based on the C_2^*/OH^*

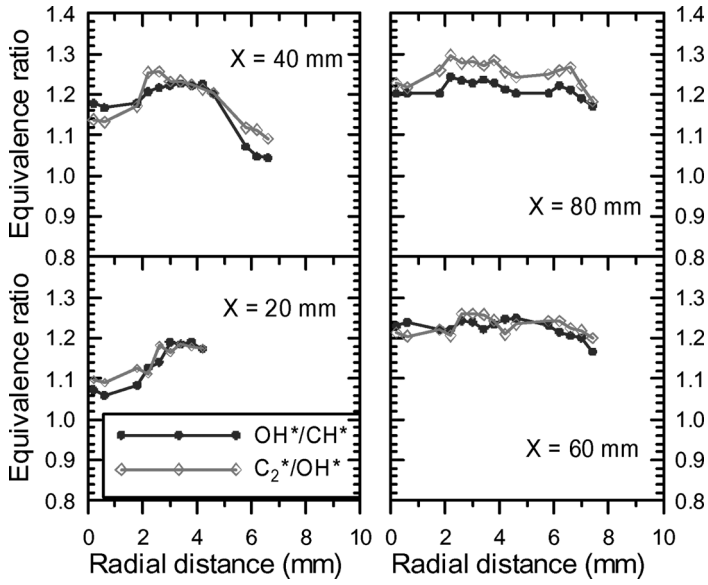

Figure 11. Time-averaged local equivalence ratio measurements at four downstream locations in a partially premixed swirling flame ($\Phi_F = 3.1$).

may be due to incomplete subtraction of the broadband background emissions. Since the C_2^* signal is obtained from the sum of the $C_2^*(0, 0)$ and $C_2^*(1, 1)$ peaks and the baseline of the $C_2^*(0, 0)$ band is not as flat as those of OH^* and CH^* bands; therefore, incomplete subtraction of the background emissions associated with CO_2^* or HCO^* may result in slightly higher C_2^*/OH^* ratio and hence higher equivalence ratio.

Nevertheless, the measured equivalence ratio is still within the experimental uncertainty (± 0.1) for the present system. These results also suggest that the intensity ratio of OH^*/CH^* is a more sensitive measure of equivalence ratio for methane flames as reported by Muruganandam et al. (2005) and Kojima et al. (2005). The measured local equivalence ratio seems reasonable because the strongly swirling air could rapidly reduce the premixed fuel-rich mixtures ($\Phi_F = 3.1$) to a leaner condition. Although multipoint measurements of local equivalence ratio in a partially premixed swirling flame have been demonstrated to be feasible, the accuracy of this technique strongly depends upon the efficiency of the detectors. Moreover, the technique seems only applicable to the reaction zone of the flames where excited species OH^*, CH^*, and C_2^* are formed.

It should be noted that the future application of this technique for spatially and temporal resolved scalar dissipation rate measurement in turbulent flames can be a great challenge in spite of simultaneous temperature measurement. The spatial resolution of the present measurement system is suitable for scalar dissipation rate measurement in turbulent flames depending on the local Kolmogorov length scale. Nandula et al. (1994) estimated that for $\Delta/\eta = 2.7$ the measurement can capture at least 90% of the scalar dissipation, and the corresponding value of $\Delta/\eta = 4.9$ is at least 75% in a turbulent jet flame at $x/D = 30$ and $Re = 15{,}600$, where $\Delta = 0.4$ mm is the spatial resolution and η is the Kolmogorov length scale. For lower Reynolds number and better resolution cases ($\Delta = 0.2$ mm), the amount of scalar dissipation captured will be higher. Although the spatially resolved measurement of scalar dissipation can be achieved, the time-resolved measurement can be a problem.

In turbulent flames, the Kolmogorov time scale ranges from less than 1 μs to 1 ms or slightly higher depending on the Reynolds number and measurement location. While the gate time of the ICCD camera must be set to 0.4 ms or longer in order to obtain the measurable chemiluminescence signal. We have examined the chemiluminescence intensity as a function of detector gate time in a rich flame ($\Phi = 1.2$) and found the minimum gate time for detectable OH^*, CH^*, and C_2^* signals to be 0.4 ms. Therefore, this technique may only be applicable to the flame region where the Kolmogorov time scale is comparable to the lifetime of chemiluminescence signal. Further assessment of the applicability of this technique for non-premixed turbulent flame measurements using other diagnostic method such as Raman scattering technique is warranted.

CONCLUSIONS

Spatially resolved, time-averaged, multipoint measurements of flame emission spectra using two Cassegrain mirrors and two spectrometers are performed and used to obtain the correlation of the intensity ratio of OH^*/CH^* and C_2^*/OH^* to the equivalence ratio in laminar methane/air flames over an equivalence ratio range of 0.8–1.4. Results demonstrate that a strong correlation exists between the intensity ratio and equivalence ratio. Curve-fitting of experimental data obtained from laminar flames is used to derive the calibration equations. The calibration equations are then applied to measure the local equivalence ratio in a

partially premixed swirling flame. Experimental results show that multipoint measurement of local equivalence ratio in the flame is feasible. However, this non-laser-based chemiluminescence technique can only be applied to determine the local flame stoichiometry in the reaction zone of partially premixed swirling methane flames. Further improvement of the sensitivity of measurement system can be achieved by using higher quantum efficiency detectors and reducing the spectral linewidths. Moreover, simultaneous measurements of equivalence ratio and temperature are possible if the signal strength of the $C_2^*(0, 0)$ and $C_2^*(1, 1)$ bands are strong enough. Therefore, one-dimensional scalar dissipation rates in partially premixed flames may be deduced to help understand the effects of mixing and combustion processes on the behavior of NO_x emissions, if the flame time scale is comparable to the lifetime of chemiluminescence signal and can be resolved by the present technique.

REFERENCES

Akamatsu, F., Wakabayashi, T., Tsushima, S., Mizutani, Y., Ikeda, Y., Kawahara, N., and Nakajima, T. (1999) The development of a light-collecting probe with high spatial resolution applicable to randomly fluctuating combustion fields. *Meas. Sci. Technol.*, **10**, 1240–1246.

Chen, R.-H. (1995) Some characteristics of NO_x emission of turbulent nonpremixed hydrogen-air flames stabilized by swirl-generated flow recirculation. *Combust. Sci. Tech.*, **110–111**, 443–460.

Cheng, T.S., Chao, Y.-C., Wu, D.-C., Yuan, T., Lu, C.-C., Cheng, C.-K., and Chang, J.-M. (1998a) Effects of fuel-air mixing on flame structures and NO_x emissions in swirling methane jet flames. *Proc. Combust. Inst.*, **27**, 1229–1237.

Cheng, T.S., Yuan, T., Chao, Y.-C., Lu, C.-C., and Wu, D.-C. (1998b) Premixed methane-air flame spectra measurements using UV Raman scattering. *Combust. Sci. Tech.*, **135**, 65–84.

Cheng, T.S., Chao, Y.-C., Wu, D.-C., Hsu, H.-W., and Yuan, T. (2001) Effects of partial premixing on pollutant emissions in swirling methane jet flames. *Combust. Flame*, **125**, 865–878.

Gaydon, A.G. and Wolfhard, H.G. (1978) *Flames: Their Structure, Radiation, and Temperature*, 4th ed., Chapman and Hall, London.

Gore, J.P. and Zhan, N.J. (1996) NO_x emission and major species concentrations in partially premixed laminar methane/air co-flow jet flames. *Combust. Flame*, **105**, 414–427.

Hardalupas, Y., Orain, M., Panoutsos, C.S., Taylor, A.M.K.P., Olofsson, J., Seyfrid, H., Richter, M., Hult, J., Aldén, M., Hermann, F., and Klingmann, J.

(2004) Chemiluminescence sensor for local equivalence ratio of reacting mixtures of fuel and air (FLAMESEEK). *Appl. Therm. Eng.*, **24**, 1619–1632.

Ikeda, Y., Kojima, J., Hashimoto, H., and Nakajima, T. (2002) Detailed local spectra measurement in high-pressure premixed laminar flame. Paper No. AIAA-2002-0191, 40 Aerospace Science Meeting and Exhibit, Reno, Nevada, January 14–17.

Ishiguro, T., Tsuge, S., Furuhata, T., Kitagawa, K., Arai, N., Hasegawa, T., Tanaka, R., and Gupta, A.K. (1998) Homogenization and stabilization during combustion of hydrocarbons with preheated air. *Proc. Combust. Inst.*, **27**, 3205–3213.

Kojima, J., Ikeda, Y., and Nakajima, T. (2000) Spatially resolved measurement of OH^*, CH^* and C_2^* chemiluminescence in the reaction zone of laminar methane/air premixed flames. *Proc. Combust. Inst.*, **28**, 1757–1764.

Kojima, J., Ikeda, Y., and Nakajima, T. (2003) Multi-point time-series observation of optical emissions for flame-front motion analysis. *Meas. Sci. Technol.*, **14**, 1714–1724.

Kojima, J., Ikeda, Y., and Nakajima, T. (2005) Basic aspect of OH(A), CH(A), and C_2(d) chemiluminescence in the reaction zone of laminar methane-air premixed flames. *Combust. Flame*, **140**, 34–45.

Lawn, C.J. (2000) Distributions of instantaneous heat release by the cross-correlation of chemiluminescent emissions. *Combust. Flame*, **123**, 227–240.

Lyle, K.H., Tseng, L.K., Gore, J.P., and Laurendeau, N.M. (1999) A study of pollutant characteristics of partially premixed turbulent jet flames. *Combust. Flame*, **116**, 627–639.

Muruganandam, T.M., Kim, B.-H., Morrell, M.R., Nori, V., Patel, M., Romig, B.W., and Seitzman, J.M. (2005) Optical equivalence ratio sensors for gas turbine combustors. *Proc. Combust. Inst.*, **30**, 1601–1609.

Nandula, S.P., Brown, T.M., and Pitz, R.W. (1994) Measurements of scalar dissipation in the reaction zones of turbulent nonpremixed H_2-air flames. *Combust. Flame*, **99**, 775–783.

Najm, H.N., Paul, P.H., Mueller, C.J., and Wyckoff, P.S. (1998) On the adequacy of certain experimental observables as measurements of flame burning rate. *Combust. Flame*, **113**, 312–332.

Roby, R.J., Hamer, A.J., Johnsson, E.L., Tilstra, S.A., and Burt, T.J. (1995) Improved method for flame detection in combustion turbines. *ASME J. Eng. Gas Turbine Power*, **117**(2), 332–340.

Roby, R.J., Reaney, J.E., and Johnsson, E.L. (1998) Detection of temperature and equivalence ratio in turbulent premixed flames using chemiluminescence. *Proceedings of the 1998 International Joint Power Generation Conference*, **1**, 593–602.

Sandrowitz, A.K., Cooke, J.M., and Glumac, N.G. (1998) Flame emission spectroscopy for equivalence ratio monitoring. *Appl. Spectrosc.*, **52**(5), 658–662.

Scott, D.A., King, G.B., and Laurendeau, N.M. (2000) Digital control of equivalence ratio using chemiluminescence feedback for a continuous combustor. *Combust. Sci. Tech.*, **159**, 129–146.

Scott, D.A., King, G.B., and Laurendeau, N.M. (2002) Chemiluminescence-based feedback control of equivalence ratio for a continuous combustor. *J. Propul. Power*, **18**, 376–382.

Terasaki, T. and Hayashi, S. (1996) The effects of fuel-air mixing on NO_x formation in non-premixed swirl burners. *Proc. Combust. Inst.*, **26**, 2733–2739.

Yamazaki, M., Ohya, M., and Tsuchiya, K. (1990) Detection of the air equivalence ratio of a burner from the flame-emission spectra. *Inter. Chem. Eng.*, **30**, 160.